

# HPC DESIGN BASED ON MULTIDISCIPLINARY NUMERICAL SIMULATION

*J. Temis, A. Selivanov, G. Yurchenko, D. Yakushev, V. Novokreshchenov*

Mathematical Simulation Department, CIAM, Moscow, Russia, tejour@ciam.ru

## ABSTRACT

The methodology to solve the interrelated problems of secondary gas flows in turbomachines, thermal and stressed states of their parts, and clearance change over a flight cycle is described using an example of high pressure compressors (HPC) of aviation engines. An iterative calculating scheme is proposed to take into account mutual interferences between these solution modules. An additional optimization module is used to minimize weight and to achieve the prescribed displacements and safety margins. Mathematical 1D and 2D models for accurate calculation of secondary flows are described in detail. The results of the application of this iterative calculation scheme for the HPC with one of the possible secondary flows design are shown. The methodology is used to estimate the efficiency of alternative secondary flows schemes with hot gas redirection to a compressor's disks hubs in order to minimize disks temperature gradients and to stabilize clearances aimed to achieve higher efficiency and gas-dynamic stability.

## NOMENCLATURE

$b_k$	size-shape factor in labyrinth seal	$\Delta P_{cpt}^*$	pressure change due to centripetal forces
$C$	empirical constant	$P_k$	static pressure in labyrinth seal cavity
$c_p$	specific heat at constant pressure	$P_i, P_j$	static pressure in the network nodes
$c$	speed of sound	Pr	Prandtl number
$d$	gap between rotor and stator surfaces in the cavity	$Q$	heat exchange flux
$e$	internal energy	$R_g$	gas-dynamic constant
$F_r, F_\varphi$	mass force in radial and circumferential direction	$r$	radius
$f_1, f_2$	dimensionless friction coefficient on the rotor and stator surfaces correspondingly	$Ra_l$	local Rayleigh number
$G_{i-j}$	flow ratio on the network branch	Re	Reynolds number
$H_k$	size-shape factor in labyrinth seal	$S$	channel sectional area
$Km$	empirical coefficient	$T$	temperature
$k_1, k_2$	conformity parameter	$t$	time
$L$	work done by rotating surface	U	radial displacement
$L_k$	size-shape factor in labyrinth seal	$V_r, V_z, V_\varphi$	gas velocity in radial, axial and circumferential direction
$l$	characteristic dimension	$W$	weight
$m$	area ratio	$Z$	vector of sealing gaps
Nu	Nusselt number	$Z_{cur}, Z_{prev}$	current and previous seals gap
$n$	empirical constant	$\alpha$	heat transfer coefficient
$P, P^*$	static and total pressure	$\beta$	swirl ratio
$\Delta P$	pressure loss	$\beta_k$	dimensionless coefficient in Chaplygin equation
		$\chi$	empirical coefficient

$\delta$	channel gap	$\sigma$	empirical coefficient
$\varepsilon$	required accuracy	$\tau_r$	friction stress in radial direction on the rotor surface
$\gamma$	adiabatic index	$\tau_{\Sigma r}, \tau_{\Sigma z}, \tau_{\Sigma \varphi}$	summarized friction stress in radial, axial and circumferential direction correspondingly
$\lambda$	conductivity coefficient	$\tau_{1z}, \tau_{2z}$	friction stress in axial direction on the rotor and stator
$\lambda'$	modified conductivity coefficient	$\tau_{1\varphi}, \tau_{2\varphi}$	friction stress in circumferential direction on the rotor and stator
$\mu$	dynamic viscosity	$\omega$	rotor angular velocity
$\mu'$	modified dynamic viscosity	$\xi$	drag coefficient
$\mu_0$	dimensionless geometric parameter	$\psi$	dimensionless geometric parameter
$\mu_k$	discharge coefficient		
$\pi(\lambda)$	pressure ratio		
$\pi$	Pi number		
$\theta$	compressibility function		
$\rho$	density		
$\rho_i, \rho_j$	density in the network nodes		

## INTRODUCTION

A modern aviation engine design process implies the usage of multidisciplinary mathematical models of the whole engine. These thermomechanical models are the pride of aviation corporations (Sun, 2008) as they provide a simultaneous solution for gas dynamics, thermal and stressed states and clearances changes over the engine flight cycle.

In spite of the significance of the problem, there are very few publications on this topic available in open literature. Most of which appeared within the last few years.

Muller (Muller, 2009) described an iteration scheme for the coupled solving of secondary gas flow parameters and deformed structural state. The solution is taken in the steady-state approach.

Arkhipov et al. (Arkhipov, 2009) proposed a cost-effective algorithm aimed to obtain clearances changes throughout the engine and full operation cycle using both 2D and 3D models. This paper combines those approaches and adds new ideas for improvement. The proposed methodology enables the following:

- obtain the accurate solution of coupled task fully described hereafter;
- perform the solution in a transient and cost-effective way;
- perform the optimization procedure based on uncommon objectives (e.g. clearances stabilization).

The main focus is on high pressure compressors. At the same time the proposed methodology is applicable to the whole engine or any part of it. Thermal and structural analyses of HPC parts need a preliminary calculation of secondary gas flows in order to obtain gas pressure, temperature and heat transfer coefficient distributions on each HPC part surface and at each of the engine operating rates. At the same time, part deformations influence gaps in seals and ducts and on secondary gas flow properties accordingly. In order to take into account this feedback an iterative solution algorithm is proposed.

The iteration process is organized as described in Fig. 1.

Typical calculations on each solution step include the following:

- hydraulic net solution in order to define the secondary flow parameters - gas temperatures, pressures and heat transfer coefficient distributions;
- 2D thermal analysis of HPC parts over the flight cycle using a convective boundary conditions of all surfaces;
- 2D HPC structural analysis at the prescribed time stamps with further determination of clearances changes;
- definition of mounting gaps, correction of boundary conditions for hydraulic net, comparison with previous iteration in order to check a stopping condition.

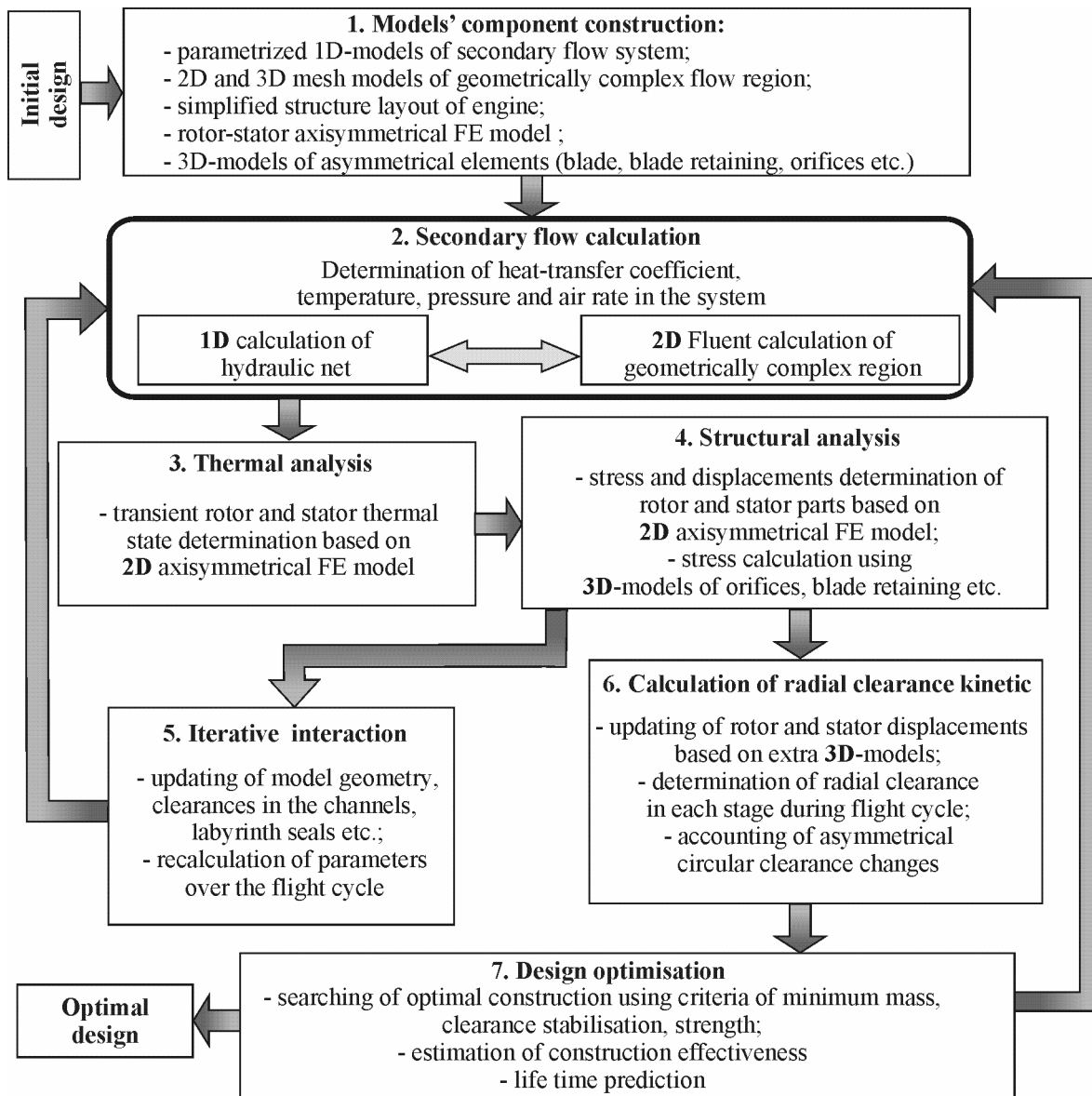


**Fig. 1. The main iterative scheme**

The most interesting part of this methodology is a secondary gas flows simulation. This procedure is based on a hydraulic net solution described below.

## SECONDARY FLOW CALCULATION

The methodology for solving secondary flows is based on building a hydraulic net and using one-dimensional flow models (Slitenko, 1994). However, there are circulatory flows in the HPC interdisk cavities for which the application of one dimensional models is ineffective. Therefore, the one-dimensional and the two-dimensional gas-dynamic models are united in the proposed calculation scheme. It enables one to obtain the distributions of heat transfer coefficient, temperature and pressure in the inter-disk cavities. This data allows for more accurate calculation of the HPC thermal and stress states.

Temperature distribution in rotor and stator parts is defined by geometry, material properties and convective heat exchange with gas flows in the main tract and in the cooling air system (secondary flows). It also takes into account the contact heat exchange between conjugated parts.

Heat exchange parameters (heat transfer coefficient and gas temperature) are the functions of flow leakage, gas velocities, density and other gas properties in the secondary flow system. These

parameters depend on the secondary flow path geometry, channels and seals gaps, hydraulic resistance coefficients, rotor angular velocity  $\omega$  and boundary conditions.

The hydraulic net method is based on a secondary air system discretization into basic elements such as: annular and radial channels, radial cavities, labyrinth seals, and elementary hydraulic resistance. One-dimensional models of the flow are developed for every type of element.

## ONE-DIMENSIONAL MODELS OF THE FLOW

One dimensional models of basic elements are described below.

### Annular Channel

The conservation equations for mass, momentum and energy written in a cylindrical coordinate system (Kochin, 1955) are used to describe the flow in an annular channel with assumption of axisymmetric flow. Moreover we are assumed the parameters aren't changed along radial direction only. Taking this assumption into consideration, we obtain the governing equation system:

$$\frac{d(\rho V_z \delta)}{dz} = 0; \quad \rho \delta V_z \frac{dV_z}{dz} = -\tau_{\Sigma z} - \delta \frac{dP}{dz}; \quad \rho \delta V_z \frac{dV_\varphi}{dz} = -\tau_{\Sigma \varphi}; \quad (1)$$

$$\frac{d(e\rho\delta V_z)}{dz} + \frac{d(P\delta V_z)}{dz} + L + Q = 0,$$

where  $\tau_{\Sigma z}$  and  $\tau_{\Sigma \varphi}$  are summarized friction stresses in axial and circumferential directions respectively;  $L$  is work done by rotating surface;  $Q$  is a heat exchange flux;  $e$  is an internal energy.

Friction stress is calculated as follows:

$$\tau_{1z} = \frac{f_1}{4} \sigma \rho \frac{V_z \sqrt{V_z^2 + (V_\varphi - R\omega)^2}}{2}; \quad \tau_{1\varphi} = \frac{f_1}{4} \sigma \rho \frac{(V_\varphi - R\omega) \sqrt{V_z^2 + (V_\varphi - R\omega)^2}}{2}; \quad (2)$$

$$\tau_{2z} = \frac{f_2}{4} \sigma \rho \frac{V_z \sqrt{V_z^2 + V_\varphi^2}}{2}; \quad \tau_{2\varphi} = \frac{f_2}{4} \sigma \rho \frac{V_\varphi \sqrt{V_z^2 + V_\varphi^2}}{2},$$

where  $\sigma$  is an empirical coefficient;  $f_1$  and  $f_2$  are dimensionless friction coefficients on the rotor and stator surfaces.

Heat transfer coefficient is computed using the equation  $\alpha = \lambda \text{Nu} / l$ , where Nu is Nusselt number determined as  $\text{Nu} = 0.021 \chi \text{Pr}^{0.43} \text{Re}^{0.8}$ , where  $\chi$  – coefficient which consider heat exchange intensification in the channel lead, Re is Reynolds number (Slitenko, 1994).

### Radial Cavity and Channel

Constitutive equations for radial cavities and radial channels have the same structure (Slitenko, 1994), but they have different expressions for mass forces ( $F_r$ ,  $F_\varphi$ ), work  $L$  and heat flux  $Q$ . Moreover they were written under the assumption that all gas-dynamic parameters were changed in the radial direction only:

$$\frac{d(\rho V_r S)}{dr} = 0; \quad V_r \frac{dV_r}{dr} - \frac{V_\varphi^2}{r} = F_r - \frac{1}{\rho} \frac{dP}{dr}; \quad V_r \frac{dV_\varphi}{dr} + V_r \frac{V_\varphi}{r} = F_\varphi; \quad (3)$$

$$\frac{d(e\rho V_r r \delta)}{dr} + L + Q = 0.$$

<i>Radial channel</i>	<i>Radial cavity</i>
$F_r = -\frac{2\tau_r}{\rho R} + r\omega^2; F_\varphi = 2\omega V_r;$	$F_r = -\frac{1}{\rho d}\tau_{\Sigma r}; F_\varphi = -\frac{1}{\rho d}\tau_{\Sigma\varphi}$

Heat transfer coefficient depends on the wall motion: for rotating wall  $Nu = 0.0196|1 - \beta|^{0.2} Re^{0.8} Km$ , where  $\beta$  is a swirl ratio; for stationary wall  $Nu = 0.037Re^{0.8}Pr^{0.33}$  (Dorfman, 1960).

### Labyrinth Seal

Investigation of the flow in a labyrinth seal shows that the flow structures in the chamber and the annual gap above it are different. Chamber flow is characterized by vortical structure, while annual gap flow has an axial direction mainly. However, pressures in these regions are practically the same. Therefore, the “two control volumes” model is used to calculate gas flow parameters through the labyrinth seal (Fig. 2).

Governing equations for annual channel, radial cavity and channel have a continuous structure, whereas the governing equation for labyrinth seals has a discrete structure.

In the axisymmetric case the constitutive equation for  $k$ -th labyrinth cavity (Childs, 1993) can be written as :

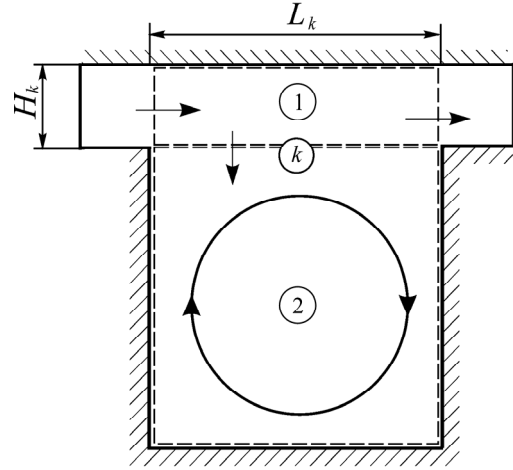


**Fig. 2. Labyrinth seal cavity**

$$\frac{\partial(P_k H_k + P_k b_k)L_k}{\partial t} + \mu_0 \mu_{k+1} H_{k+1} \sqrt{R_g T (P_k^2 - P_{k+1}^2)} - \mu_0 \mu_k H_k \sqrt{R_g T (P_{k-1}^2 - P_k^2)} = 0, \quad (4)$$

where  $\mu_0 = (1 - \psi)^{-0.5}$ , with  $\psi$  is a dimensionless geometric parameter. Discharge coefficient  $\mu_k$  is determined by Chaplygin equation (Childs, 1986 and 1993) as  $\mu_k = \pi / (\pi + 2 - 5\beta_k + 2\beta_k^2)$ , where  $\beta_k = -1 + (P_{k-1} / P_k)^{(\gamma-1)/\gamma}$ .

### Elementary Hydraulic Resistance

Elementary hydraulic resistance is used for sudden expansion channels. In this case the drag coefficient depends on the cross-section area ratio  $m$  and is computed by Bordo-Carnot formula  $\xi = (2\Delta P) / \rho V^2 = (1 - m)^2$ , where  $\Delta P$  – pressure loss (Idelchik, 1960).

### BASIC ELEMENTS VERIFICATION

Computational modules were developed and implemented in the Maple software for all described basic elements. These modules are integrated into the common program, which allows automated hydraulic net processing. The fourth order Runge-Kutta method is used for solving nonlinear differential equations.

Verification of 1D models of basic elements was performed in the Fluent software. 2D and 3D CFD verification models were developed for each basic element. In the 2D and 3D CFD calculation the mesh quality parameter  $Y^+$  was less than 3. This allows use of  $k - \varepsilon$  turbulence model and a two-layer model for enhanced wall treatment (for more specification see Fluent documentation).

The same types of boundary conditions (pressure, temperature, swirl) were specified for 1D models and CFD verification models. Values of gas-dynamic parameters are same as in typical HPC.

Relative error of pressure (to pressure drop between inlet and outlet) for annual channel flow is about 4%; for radial channel flow – 3.9%; for radial cavity – 4.6%. Absolute error for outlet temperature in the annual channel is 0.9 K; in the radial channel – 1.2 K; in the radial cavity – 2.5 K. Absolute error for radial velocity in the annual channel is 3.7 m/s; in the radial channel – 4.2 m/s; in the radial cavity – 3.1 m/s.

Obtained results show that 1D models are suitable for engineering calculations.

## 2D MODELS OF CAVITIES

1D models can be used for radial cavities with through flow, but for closed HPC cavities with circular flow it is necessary to use 2D models. This approach is proposed in (Kadaner, 2001), but in that work cavities were considered isolated regions without connection with other secondary flow system elements. In present work, the 2D cavity models and 1D hydraulic net models are united into the computation algorithm.

2D model contains main region I and connection region II joined to the shaft (Fig. 3). At the same time region II included as a branch (annual channel with zero friction on the upper wall) into the global hydraulic net. 1D and 2D models are glued together by matching boundary conditions. After finishing the initial calculation of hydraulic net, the obtained parameters are transferred to the 2D cavity model as boundary conditions. 2D simulations are carried out and then a hydraulic net model is adopted if it is necessary.

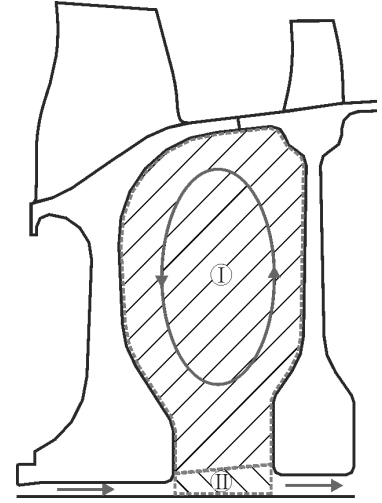


Fig. 3. Cavity model

It should be noted that 3D flow structures have been experimentally observed in the HPC cavities. They are driven by a “buoyancy effect”: regions of gas with different temperatures shifting in a mass force (Bohn and Deutsch, 2005). However, for engineering calculations these 3D models are impractical due to computational costs. A probable solution is to modify a viscosity as  $\mu' = CRa_l^n \mu$  and heat conductivity coefficient as  $\lambda' = CRa_l^n \lambda$  in a 2D model, where  $C$  and  $n$  are empirical constants;  $Ra_l$

is a local Rayleigh number which calculated as:  $Ra_l = Pr \frac{\rho^2 \omega^2 l^4}{\mu^2} \max \left( \left( \frac{\omega r}{c} \right)^2 - \frac{r}{\rho} \frac{d\rho}{dr}, 0 \right)$ , where

$Pr = \mu c_p / \lambda$  – Prandtl number;  $c_p$ ,  $\rho$ ,  $c$ ,  $\omega$ ,  $l$ ,  $r$  – specific heat at constant pressure, density, speed of sound, rotational velocity, characteristic dimension and radius respectively. More detailed information can be found in (Kilfoil and Chew, 2009).

## HYDRAULIC NET BUILDING

Hydraulic net creation is performed by dividing secondary flow system into basic elements which form branches, connected to each other by nodes.

The second Kirchhoff law for flow ratios is applied to every inner node:

$$\Sigma G_{i-j} = 0. \quad (5)$$

Binding pressure equation for end nodes  $i$  and  $j$  of every branch may be written as (Slitenko, 1994; Kharkovskiy, 1990):

$$P_i / \pi(\lambda_i) - P_j / \pi(\lambda_j) = \xi \theta G_{i-j}^2 / (2\rho_j S^2) \pm \Delta P_{cpl}^*, \quad (6)$$

where  $\pi(\lambda) = P / P^*$ ;  $P$  is a static pressure,  $P^*$  is a total pressure,  $\Delta P_{cpt}^*$  is a pressure change due to centripetal forces,  $S$  – flow sectional area;  $G$  – flow ratio in net branch;  $\theta$  – compressibility function (Dorfman, 1960).

Unknown values of net nodal pressures can be found by solving the set of nonlinear equations using a successive approximations method.

## THERMAL AND STRESS STATE CALCULATIONS AND CLEARANCES EVALUATION

Obtained gas temperature, pressure and heat transfer coefficient distributions on all parts' surfaces (in 2D) for main engine operation rates are transferred to the next calculating module according to the global iteration process scheme (see Fig. 1). This transferring is done by a Maple script which reads data from text files and produces tables for ANSYS thermal boundary conditions affixing. Thus, all transitional operation rates utilize a linear approximation of available data. Gas parameters in the main flow are supposed to be fully defined.

The HPC rotor and case thermal solution is carried out by ANSYS in a 2D axisymmetric transient approach using material thermal nonlinearities. Obtained parts' temperature distributions are saved for future use in structural analysis.

Structural analysis is performed in a 2D axisymmetrical formulation. Some HPC parts, i.e. blades and disk's bolted joint zones, are modeled using plane-stress elements with thickness. Solution is done using the quasi-stationary approach with geometrical and physical nonlinearities (i.e. large displacements and plasticity). Loading factors are rotational speed, thermal loads, pressure on parts surfaces and axial forces on blades. All of which are operation rate-dependent.

By performing structural solution it becomes possible to determine the rotor and case displacements through the whole flight cycle, changes to radial clearances, and to evaluate a static safety margin and cyclic durability.

Sealing clearances values, which determines the secondary flow ratios, are transferred to the input of the first calculation block of the iterative scheme as a text file in order to perform the next iteration. By defining  $Z_{cur}$  as a vector of sealing gaps obtained from the last iteration at the used time stamps and  $Z_{prev}$  as values from the previous iteration, it can be evaluated a condition of iteration stoppage in the form

$$\|Z_{cur} - Z_{prev}\| / \|Z_{prev}\| < \varepsilon, \quad (7)$$

where  $\varepsilon$  is a required accuracy. For most applications it can be set to  $10^{-2}$  ...  $10^{-3}$ .

The described methodology found an application in the design process of several perspective engines in Russia. In particular, by performing this calculation it becomes possible to estimate the effect of a new schemes of secondary flows redirection from a last HPC stage's main flow to hubs of a rear HPC stages disks. It helps to minimize disk temperature gradients and to stabilize radial clearances above the blades and in sealings through the flight cycle in order to achieve a higher efficiency factor and gas-dynamic stability of operation.

Below there is an example of the methodology applied to calculation of the HPC, shown in Fig. 4, which is characterized by a relatively simple hydraulic net. Rotor radial displacements distribution at take-off conditions with a scale factor 10 is shown in Fig. 5.

Rear HPC sealing gap affects secondary flow ratios as it regulates one of the net branches. The sealing gap changes, scaled to a certain value  $\Delta U^*$  to clarify the comparison and plotted over the whole flight cycle after the first and the second iterations, are shown in Fig. 6. There are possible sealing mounting gap values on the graphs, which are significantly different between iterations.

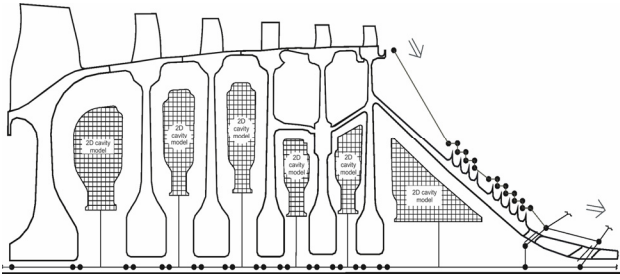


Fig. 4. HPC hydraulic net

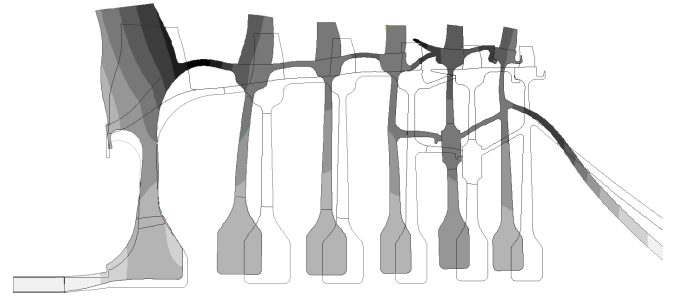


Fig. 5. HPC rotor radial displacements at take-off (scale factor 10)

Zero level on these graphs corresponds to initial state with no rotation and uniform temperature. Calculations were done from the ground idling conditions through the ordinary engine flight cycle, including ground maneuvers (0-0.08 relative time), take-off (0.08-0.09), climb (0.09-0.32), cruise (0.32-0.73), descent (0.73-0.89), landing (0.89-0.95) and reverse (0.95-0.96).

On one hand, it is important to choose the mounting gap so that there will be no contact. On the other hand, excessive gaps cause a considerable drop in efficiency and gas-dynamic stability. First of all, it is necessary to accurately solve the multidisciplinary problem of clearance changes, and then it becomes possible to make some improvements and to perform an optimization procedure.

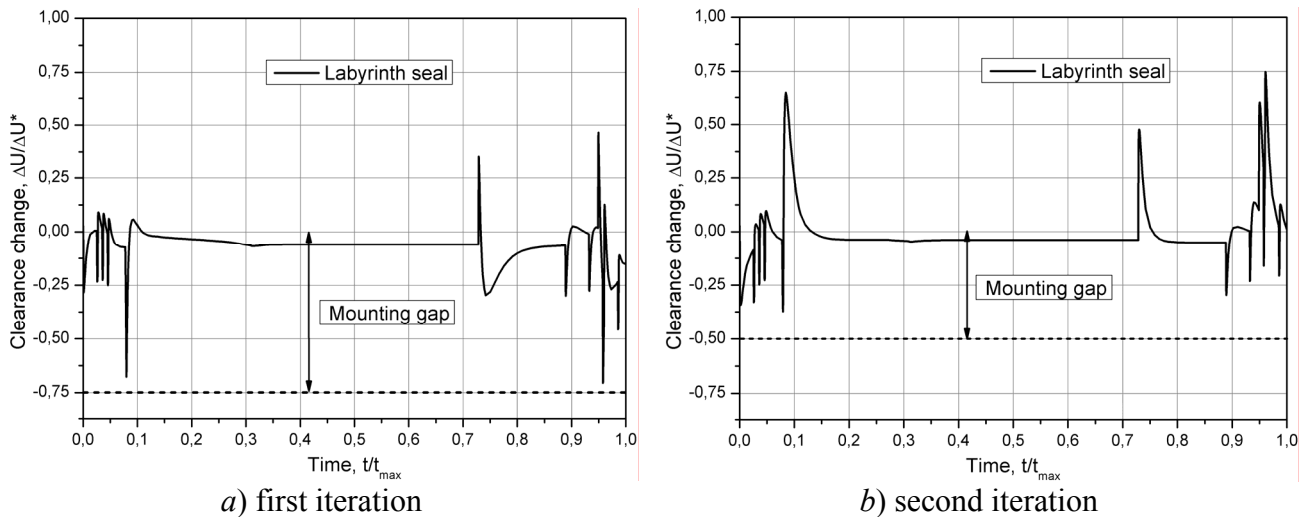


Fig. 6. Seal clearance changes

## DESIGN OPTIMIZATION

The common optimization goal is to reduce the weight (Temis, 2010), but combining with proposed cost-effective techniques, we can also optimize to achieve predefined cycling strength, blade tip clearance values and other targets.

The problem of radial clearance minimization is solved with both changing disk temperature distribution and disk stiffness optimization. The preliminary design of rotor and stator with approximate displacements gives the desired radial clearances. For this rotor design it is necessary to calculate weight-stiffness dependence of optimal disks. The disk optimization allows obtaining necessary construction stiffness with the stress restriction and high reliability which are required.

The goal of disk optimization problem is to minimize the disk weight under certain stress and displacement constraints by disk shape changing. The disk minimization problem is solved under take-off loads and thermal load which calculated in the thermal analysis procedure. The first stage compressor blisk optimization is considered as an example. Disk shape parametrization is used in the optimization process. A 2D parameterized finite element model is used in order to speed-up the optimization process. The disk model uses axisymmetric finite elements; blade model uses plane-

stress finite elements with variable thickness. Blade and rim areas are not varied. Disk shape is defined by geometric parameters of two splines. Each spline has four parameters which define disk thickness at various radial locations. Technological and constructive constraints which determine parameters limits are also considered. Constraints on radial and axial displacements of rim disk provide the desired stiffness. Constraint on maximal stress provides the desired safety margin. The dependence between optimal disk weight and permissible rim radial displacement is shown in Fig. 7. The disk becomes more lightweight when permissible rim radial displacement constraint is increased. For disks with low stiffness, stress constraints become an essential requirement which limits further stiffness reduction.

The computer-aided design software with methods of optimal design can provide some considerable results. The in-house software includes finite element analysis procedure and optimization procedure with sequential quadratic programming (SQP) algorithm (Schittkowski, 1985). The optimization software consists of several modules which solve various tasks. One of these modules is a control program which performs interaction between modules. The control program starts each module in determined order, processes data flows between geometry, finite element analysis and result modules. This program includes an interactive graphical environment which allows defining initial data, design parameters, objective function, constraints, to control and operate the optimization process. Optimization module modifies design parameters using SQP algorithm as search procedure. The values of objective function and constraints are calculated in finite element analysis procedure. The calculation of function gradients for SQP algorithm uses forward difference. The control program also includes a termination criterion of iteration process.

In another example, disk shape optimization with different thermal loads is considered. Last compressor stage disk has significant temperature differences between rim and hub during take-off. This thermal loads cause significant thermal stress which can be reduced by disk shape changing. Temperature difference can also be reduced by disk hub heating. The objective function of the disk optimization problem is the disk weight, which is minimized under certain stress constraints and thermal loads. Dependence between optimal disk weight and temperature difference between rim and hub is shown in Fig. 8. In this example decreasing temperature difference by 11% causes disk weight to decrease by 15%. So accurate multidisciplinary calculation of thermal loads allows for optimal disk design.

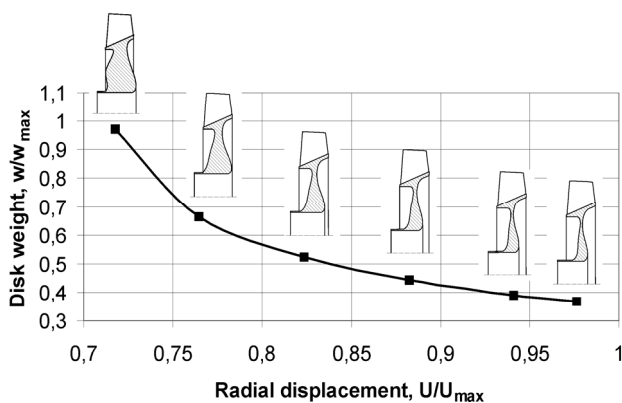


**Fig. 7. Weight-stiffness dependence of optimal disks**

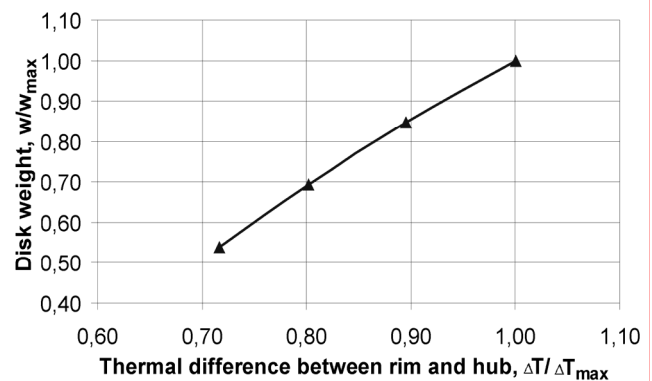


**Fig. 8. Disk weight optimization with different thermal loads**

## CONCLUSIONS

An iterative calculation scheme is proposed to solve interrelated design tasks such as secondary flows calculations, thermal and stress states evaluation and clearances changes in a more accurate way. The hydraulic net solution is noteworthy. A connection between 1D and 2D elements of the net is described as well as all of the 1D basic elements used. The proposed methodology can be used in

turbomachine design process to predict safety margins, cyclic durability, gas-dynamic efficiency and operational stability.

On the upper design level an optimization approach is described. The problem of disk optimization under certain constraints on weight, stress and radial displacement is investigated by using an in-house finite element analysis program connected with the sequential quadratic programming (SQP) algorithm in optimization procedure.

## REFERENCES

Sun, Z., Hills, N.J., Chew, J.D., Volkov, K.N., Barnes, C.J., (2008), Efficient FEA/CFD thermal coupling for engineering applications // Proc. of ASME Turbo Expo 2008, GT2008-50638, 11 p.

Muller, Y., (2009), Integrated fluid network- thermomechanical approach for the coupled analysis of a jet engine // Proc. of ASME Turbo Expo 2009, GT2009-59104, 10 p.

Arkhipov A.N., Karaban V.V., Putchkov I.V., Filkorn G., Kieninger A., (2009), The whole-engine model for clearance evaluation // Proc. of ASME Turbo Expo 2009, GT2009-59259, 9 p.

Bohn D., Deutsch G., Simon B., Burkhardt C., (2005), "Flow visualization in a rotating cavity with axial throughflow" / D. Bohn, G. Deutsch, B. Simon, C. Burkhardt // ASME Turbo Expo 2005, paper № 2000-GT-280.

Childs D.W., (1993), "Turbomachinery Rotordynamics: phenomena, modeling, and analysis" / D.W. Childs // John Wiley & Sons Inc.

Childs D.W., Scharrer J., (1986) "An Iwatsubo-Based Solution for Labyrinth Seals: Comparison to Experimental Results" / D.W. Childs, J. Scharrer // ASME Journal of Engineering for Gas Turbines and Power, 1986, pp. 325–331.

Dorfman, L.A., (1960), "Hydrodynamic resistance and heat emission of rotating bodies" / L.A. Dorfman. – Moscow: Physico-mathematical publishing house.

Idelchik, I.E., (1960), "Hydrodynamic resistance handbook" / I.E. Idelchik. – Moscow: State energy publishing house.

Kadaner, I.S., (2001), "Air flow and convective heat exchange in rotor inter-disk cavities of compressor" / I.S. Kadaner, Yu.M. Temis, L.f. Grishina // Aviation engine engineering. CIAM, 2001, paper № 1 (1320), pp. 24-36.

Kharkovskiy, S.V., (1990), "Calculating determination parameters of medium in branch air-feed system of turbine and boundary condition of heat exchange on disc surface" / S.V. Kharkovskii, V.K. Kostezh // Transaction of CIAM, 1269, – pp. 116-128.

Kilfoil A.S.R., Chew J.W., (2009), "Modeling of Buoyancy-Affected Flow in Co-rotating Disk Cavities" / A.S.R. Kilfoil, J.W. Chew // Proceedings of ASME Turbo Expo 2009: Power for Land, Sea and Air GT2009, June 8-12, 2009, Orlando, Florida, USA / GT2009-59214.

Kochin N.E., (1955), "Theoretical hydromechanics, part I and II" / N.E. Kochin, I.A. Kibel', N.V. Rose – Moscow: Government publishing house of techno-theoretical literature.

Slitenko, A.F., (1994), "Construction and calculation of GTE cooling system" / A.F. Slitenko, S.Z. Kopelev. – Kharkov: Publishing house "Osnova" under Kharkov state university.

Temis Yu.M., Yakushev D.A. Design optimisation of GTE constructive elements. Mechanical Engineering. Encyclopaedia. Aircraft and helicopter. IV-21. Aero-engine B.3. Moscow: Mashinostroenie, 2010. 570-579 pp. (in Russian).

Schittkowski K. NLPQL: A Fortran Subroutine Solving Constrained Nonlinear Programming Problems. Annals of Operation Research, 1985.